Journal of Organometallic Chemistry 695 (2010) 1328–1336

Contents lists available at ScienceDirect

Journal of Organometallic Chemistry

journal homepage: www.elsevier.com/locate/jorganchem

Pentabenzylcyclopentadienyl molybdenum and tungsten hydrides: Syntheses, structures and electrochemistry of $[MHCp^{Bz}(CO)_2(L)]$ (L = CO, PMe_3, PPh_3)

M. Augusta Antunes [a], Sónia Namorado [a], Cristina G. de Azevedo [a], M. Amélia Lemos [b], M. Teresa Duarte [a], José R. Ascenso [a], Ana M. Martins [a,*]

[a] Centro de Química Estrutural, Instituto Superior Técnico, Av. Rovisco Pais 1, 1049-001 Lisboa, Portugal
[b] IBB – Institute for Biotechnology and Bioengineering, CEQB, Instituto Superior Técnico, Av. Rovisco Pais 1, 1049-001 Lisboa, Portugal

ARTICLE INFO

Article history:
Received 3 December 2009
Received in revised form 4 February 2010
Accepted 13 February 2010
Available online 20 February 2010

Keywords:
Molybdenum
Tungsten
Hydride
Metallocenes
Cyclic voltammetry
Electrochemistry

ABSTRACT

Complexes $[MHCp^{Bz}(CO)_2(PR_3)]$ (R = CH_3, M = Mo (**1**); M = W (**2**); R = Ph, M = Mo (**3**); $Cp^{Bz} = C_5(CH_2Ph)_5$) were prepared by thermal decarbonylation of the corresponding $[MHCp^{Bz}(CO)_3]$ in the presence of trimethyl- or triphenyl-phosphine. In solution the NMR spectra of all compounds show the presence of cis and trans isomers that interconvert at room temperature. In the solid state the molecular structures obtained for compounds **1** and **2** correspond to the trans isomers, while for **3** the cis isomer is present.

The electrochemistry of $[MoHCp^{Bz}(CO)_2(PMe_3)]$ (**1**), $[MoHCp^{Bz}(CO)_3]$ (**5**), $[WHCp^{Bz}(CO)_3]$ (**6**), $[WCp^{Bz}(CO)_3]_2$ (**7**), and $[MCp^{Bz}(CO)_3(CH_3CN)]BF_4$ (**8**), is described. The cleavage of M–H bonds takes place upon oxidation or reduction. Cations $[MCp^{Bz}(CO)_2L(CH_3CN)]^+$ form in solvent-assisted M–H bond breaking upon oxidation of $[MHCp^{Bz}(CO)_2L]$ (L = PMe_3, CO). Reduction of $[MHCp^{Bz}(CO)_3]$ gives $[MCp^{Bz}(CO)_3]^-$ and H_2. The presence of one PMe_3 ligand lowers the reduction potential and precludes the observation of reduction waves.

1. Introduction

Transition metal hydrides play an important role in several stoichiometric and catalytic reactions involving the transfer of hydrogen to unsaturated organic substrates [1]. The delivery of hydrogen may occur in the form of a proton, a hydrogen atom or a hydride and methods to obtain free energy values $\Delta G^\circ_{H^+}$, $\Delta G^\circ_{H\cdot}$ and $\Delta G^\circ_{H^-}$ for a series of metal hydrides have been described [2–9]. On the other hand, the kinetic rate constants for hydride or hydrogen atom transfer were measured using the trityl cation/radical as acceptors [6,10–12].

The sequential transfer of one proton and one hydride is the basis of ionic hydrogenation reactions. The procedure was used in stoichiometric reactions to reduce unsaturated carbon–carbon, carbon–oxygen and carbon–nitrogen bonds, using strong acids and a silane or a transition metal hydride as hydride donor reagents [13–17]. Yet, in spite of proton transfer has long been identified as a current reactivity pattern for transition metal hydrides, using of this reaction in catalytic ionic hydrogenations is a recent attainment [18–21]. A catalytic hydrogenation cycle for the ionic hydrogenation of simple ketones to alcohols using as catalysts $[MoHCp(CO)_2(PR_3)]$ (R = Me, Ph, Cy) and analogous C_2- and C_3-bridged cyclopentadienyl-phosphine complexes was reported by Bullock and co-workers [22,23], and an extension of this system to $[MoHCp^{Bz}(CO)_3]$ ($Cp^{Bz} = C_5(CH_2Ph)_5$) as a catalyst precursor for ketone hydrogenation was recently made by some of us [18]. The pentabenzylcyclopentadienyl system is less prone to deactivation than the cyclopentadienyl derivatives and DFT calculations identified the active species regeneration (iv and v in Chart 1) as the slow elementary steps, leading to the conclusion that the best catalytic performance is related to the high steric bulk created by the Cp^{Bz} ligand.

The most common procedure to generate cationic transition metal hydrides is the one-electron oxidation of 18-electron neutral complexes. The electron removal is accompanied by a drastic pKa decrease [24] and therefore the 17-electron species suffer deprotonation. The proton may be captured by the medium, namely a base, the solvent or traces of H_2O, or by the neutral hydride that may itself be susceptible to protonation, leading to cationic dihydrogen or dihydride compounds [25–28]. Electrochemical studies of half-sandwich molybdenum and tungsten complexes have received considerable attention and it was reported that subsequently to deprotonation, the 17-electron radicals may be trapped by the solvent and further oxidised or dimerize through radical coupling [24,29–42].

The work reported now focuses on the syntheses and electrochemical study of new pentabenzylcyclopentadienyl molybdenum and tungsten hydride complexes. It aims the comparison with analogous cyclopentadienyl complexes described in the literature,

* Corresponding author. Tel.: +351 218419172.
E-mail address: ana.martins@ist.utl.pt (A.M. Martins).

0022-328X/$ - see front matter © 2010 Elsevier B.V. All rights reserved.
doi:10.1016/j.jorganchem.2010.02.012

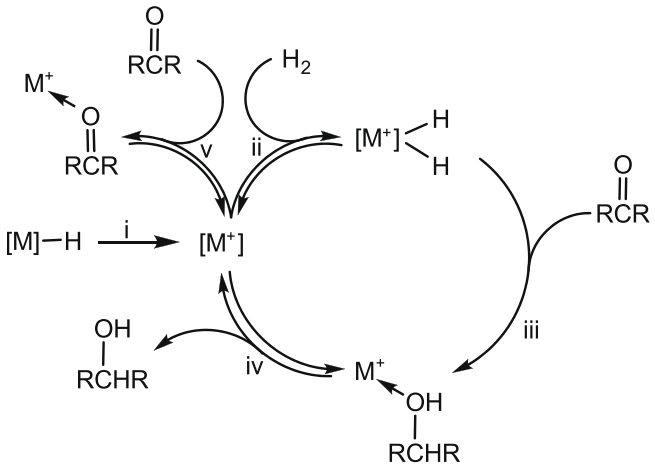

Chart 1.

and assessing the influence of a very bulky cyclopentadienyl ligand on the compounds reactivity and properties [43,44].

2. Results and discussion

2.1. Syntheses and characterisation

2.1.1. $[MHCp^{Bz}(CO)_2(PR_3)]$ complexes

Complexes $[MHCp^{Bz}(CO)_2(PR_3)]$ (R = CH_3, M = Mo (**1**); M = W (**2**); R = Ph, M = Mo (**3**); $Cp^{Bz} = C_5(CH_2Ph)_5$) were prepared in toluene by thermal decarbonylation of the corresponding $[MHCp^{Bz}(CO)_3]$ [30] in the presence of trimethyl- or triphenylphosphine. This is a common method for the replacement of one carbonyl ligand in molybdenum and tungsten half-sandwich tricarbonyl complexes that usually gives high product yields. Compounds **1**, **2** and **3** were obtained in crystalline forms after work-up in 75%, 80% and 76% yields, respectively.

The IR carbonyl stretching bands of **1**–**3** are presented in Table 1 in comparison with values reported for analogous complexes. The lower ν_{CO} values revealed by the IR spectra of **1**, **2** and **3** are consistent with the results obtained for other pentabenzylcyclopentadienyl molybdenum and tungsten compounds [30,44] and attest a more extensive metal–carbonyl back bonding in Cp^{Bz} complexes in comparison with Cp and Cp^* analogues.

On the other hand, the observation of only two CO peaks, instead of four, suggests the formation of only one isomer. The IR patterns observed in KBr are compatible with the presence of the trans isomers as the most intense peaks appear at higher wavenumbers [38]. In solution, however, the proton NMR spectra of $[MHCp^{Bz}(CO)_2(PR_3)]$ attest for the presence of cis and trans isomers. The proton NMR spectrum of **1** in C_6D_6 at room temperature shows two resonances, at δ −5.71 (br) and −5.49 (s) ppm assignable to two different hydride ligands. A variable temperature ^1H NMR study performed in d_8-toluene showed that the two resonances appearing at room temperature split in two doublets on cooling until −80 °C (Fig. 1). The multiplicity of these signals is due to the coupling with the phosphorus and the values of $^2J_{PH}$, which are 71.2 and 24.1 Hz, allow their assignment to the cis and trans isomers respectively. At room temperature the ^{31}P NMR spectrum of **1** displays one broad resonance at δ 10.9 ppm that splits in two apparent singlets at δ 19.4 (cis) and 17.0 (trans) at −80 °C. The proton resonances attributable to the Cp^{Bz} and the PMe_3 ligands broad when the temperature is lowered but do not resolve until −80 °C.

At room temperature the hydride resonance of **2** appears as a doublet of triplets at δ −7.00 ppm due to the coupling with the tungsten ($^1J_{WH}$ = 24.9 Hz) and the phosphorus ($^2J_{PH}$ = 73.6 Hz) nucleus. The PMe_3 proton resonance shows as a doublet with $^2J_{PH}$ = 8.8 Hz and the ^{31}P resonance is observed at δ −20.8 ppm as a triplet with $^1J_{PW}$ = 125.2 Hz. On cooling the solution to −80 °C the hydride resonance splits in two at δ −6.52 ppm (d, $^2J_{PH}$ = 22.6 Hz) and −6.85 ppm (dt, $^2J_{PH}$ = 72.7 Hz, $^1J_{WH}$ = 25.3 Hz). The values of the coupling constants to the phosphorus allow the assignment of the high field resonance to the cis isomer and the other to the trans isomer. At −80 °C the remaining signals are still not resolved appearing as broad resonances. The carbonyl carbon resonances of either **1** or **2** have not been detected regardless of the temperature. The phosphorus NMR resonance at δ 66.5 ppm in $[MoHCp^{Bz}(CO)_2(PPh_3)]$ (**3**), confirms the coordination of phosphine. As described for **1** and **2**, the NMR spectra of **3** show the presence of cis and trans isomers when the temperature is lowered below −30 °C. At −50 °C the hydride resonance of cis-$[MoHCp^{Bz}(CO)_2(PPh_3)]$ gives rise to a doublet centered at δ −4.52 ppm ($^2J_{PH}$ = 71.2 Hz) and that of the trans isomer appears as a doublet at δ −5.35 ppm ($^2J_{PH}$ = 20.4 Hz). The carbonyl carbon resonances are not visible in the ^{13}C NMR spectrum at room temperature but at −50 °C they give rise to one doublet at δ 246.8 ppm ($^2J_{PC}$ = 21 Hz) assigned to the CO ligand

Table 1
IR carbonyl stretching bands of **1**, **2** and **3** and values reported for analogous complexes.

Compound	$\nu_{C\equiv O}$ (cm^{-1})
$[MoHCp^{Bz}(CO)_2(PMe_3)]$, **1**	1915, 1819
$[WHCp^{Bz}(CO)_2(PMe_3)]$, **2**	1909, 1809
$[MoHCp^{Bz}(CO)_2(PPh_3)]$, **3**	1932, 1847
cis-$[MoHCp(CO)_2(PMe_3)]$ [45]	1947, 1864
trans-$[MoHCp^*(CO)_2(PMe_3)]$	1938, 1864
cis-$[MoHCp^*(CO)_2(PMe_3)]$ [46]	1938, 1860
trans-$[MoHCp^*(CO)_2(PMe_3)]$	1926, 1852
cis-$[WHCp(CO)_2(PMe_3)]$ [47]	1941, 1855
trans-$[WHCp^*(CO)_2(PMe_3)]$	1933, 1855
cis-$[WHCp^*(CO)_2(PMe_3)]$ [46]	1930, 1853
trans-$[WHCp^*(CO)_2(PMe_3)]$	1920,1843
cis-$[MoHCp(CO)_2(PPh_3)]$ [48]	1991, 1876
trans-$[MoHCp(CO)_2(PPh_3)]$ [49]	1940, 1862
cis-$[WHCp(CO)_2(PPh_3)]$ [45]	1944, 1865
trans-$[WHCp(CO)_2(PPh_3)]$	1944, 1865

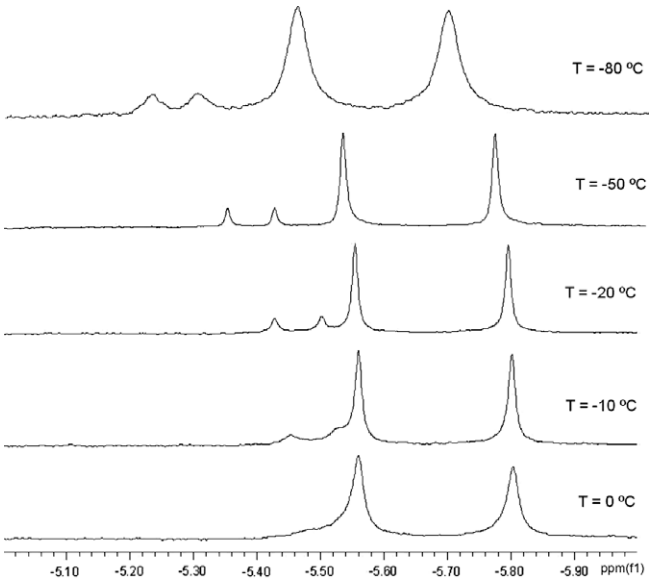

Fig. 1. A variable temperature ^1H NMR spectrum in d_8-toluene for **1**.

cis to the phosphine and one singlet at δ 238.5 ppm due to the trans CO ligand [22].

The reaction of $[MoHCp^{Bz}(CO)_3]$ with PCy_3 was performed in toluene under reflux, in experimental conditions similar to those used for the syntheses of **1**–**3**. The product isolated at the end of the reaction in 10% yield was identified by X-ray diffraction as $[Mo(CO)_4(PCy)_2]$ (**4**). A tentative explanation for the formation of **4** may involve the reductive elimination of HCpBz from the putative $[MoHCp^{Bz}(CO)_2(PCy_3)]$, forced by the bulkiness and strong donor properties of the tricyclohexylphosphine ligand, followed by reaction with CO and PCy_3. Indeed, in addition to **4**, the proton NMR spectrum of the reaction crude showed resonances characteristic of pentabenzilcyclopentadiene.

The molecular structures of complexes **1**–**4** have been obtained by single crystal X-ray diffraction. The molecular structure of **4** displays an octahedral Mo center with trans-PCy_3 ligands as reported before [50] and does not justify further discussion.

Crystals of $[MoHCp^{Bz}(CO)_2(PMe_3)]$ (**1**), $[WHCp^{Bz}(CO)_2(PMe_3)]$ (**2**), and $[MoHCp^{Bz}(CO)_2(PPh_3)]$ (**3**), were grown from Et_2O solutions cooled at −20 °C. The molecular structures are shown in Figs. 2, 3 and 4 and selected bond lengths and angles are presented in Table 2.

The first note to address about the molecular structures obtained is the fact that compounds **1** and **2**, presenting the PMe_3 ligand, correspond to the trans isomers, in spite of NMR spectra have revealed that the major species in solution are the cis isomers. The structure of **3** presents the cis isomer co-crystallized with a diethylether molecule.

In all compounds the metal coordination geometry is a distorted four-legged piano stool with angles within the expected values (see Table 2) [44,51] and thus, the Cp^{Bz}(centroid)–M–L(i) angles are higher than the corresponding L(i)–M–L(i) basal angles. They also follow the "angular trans influence" defined by Poli, which establishes that the two larger (or smaller) Cp^{Bz}(centroid)–M–L(i) angles are defined by opposite L(i) basal ligands [52b]. For all complexes the phenyl rings of four benzyl fragments are directed opposite to the metal and one is bended towards the metal but sufficiently far apart to prevent any bonding interaction. To better characterize the relative conformation of the phenyl rings we present in Table 2 the torsion angles of the pending benzyl arms defined as $M—C_{(Cp^{Bz}\ ring)}—C_{(CH_2\ bridge)}—C_{ipso}$. In all compounds the phenyl rings bending towards the metal define torsion angles of 47–50, while the others present angles that range from 155 to 177°.

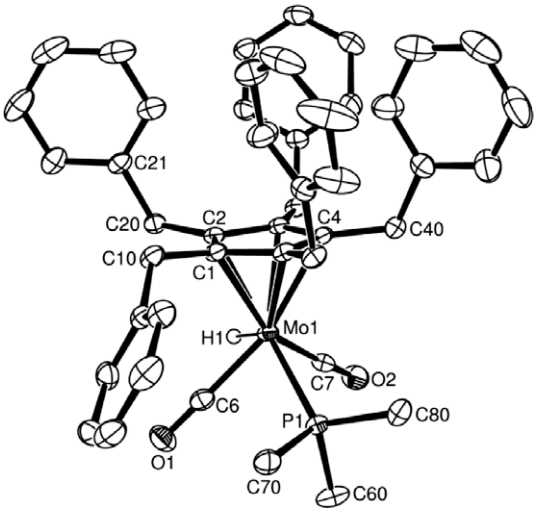

Fig. 2. ORTEP III diagram of **1**, showing the overall geometry. 50% probability level ellipsoids were used and calculated hydrogen atoms have been omitted for clarity.

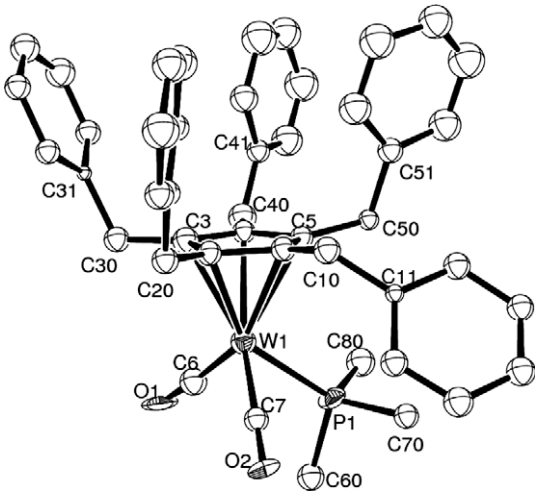

Fig. 3. ORTEP III diagram of **2**, using 50% probability level ellipsoids. Calculated hydrogen atoms have been omitted for clarity.

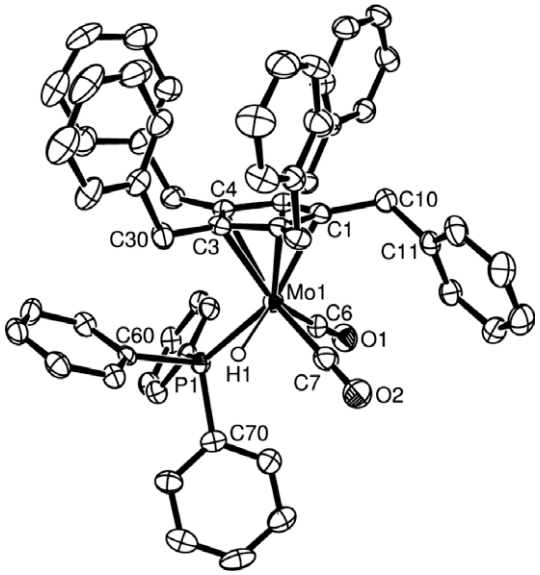

Fig. 4. ORTEP III diagram of **3**, using 50% probability level ellipsoids. Calculated hydrogen atoms have been omitted for clarity.

Compounds **1** and **2** are isostructural. The angles between the carbonyl and the hydride are narrow than CO–PMe_3 angles in consequence of the high steric bulk of trimethylphosphine. The distances M(1)–C(6), M(1)–C(7), M(1)–P(1), M(1)–H and M(1)–Cp^{Bz}(centroid) are consistent with the values reported for analogous complexes [44,52]. The benzyl substituents point towards the metal over one of the carbonyl ligands, with torsion angles C(1)–Cp^{Bz}(centroid)–Mo(1)–C(6) and C(1)–Cp^{Bz}(centroid)–W(1)–C(7) of 23.9(6)° and 28.8 (8)° in **1** and **2**, respectively. This arrangement is often observed in $[MCp^{Bz}(CO)_3X]$ (X = H, Me, Cl, I, OTf, $MCp^{Bz}(CO)_3$) complexes [18,30,44,53].

The structure of $[MoHCp^{Bz}(CO)_2(PPh_3)]$ (**3**), presents two adjacent carbonyl ligands with an angle of 81.15(18)°, comparable to those observed in $[MoHCp^{Bz}(CO)_3]$ [30]. The relative positioning of the benzyl substituents of Cp^{Bz} in relation to the basal ligands in **3** differs from the two trimethylphosphine analogues previously discussed as the benzyl group bending towards the molybdenum atom is positioned between the two adjacent carbonyl ligands with torsion angles C(1)–Cp^{Bz}(centroid)–Mo(1)–C(6) and

Table 2
Relevant bond distances (Å) and angles (°) for compounds **1**, **2** and **3**.

	[$MHCp^{Bz}(CO)_2(PMe_3)$]		[$MoHCp^{Bz}(CO)_2(PPh_3)$], **3**
	1(M = Mo)	**2**(M = W)	
M–H(1)	1.782(3)	1.702(19)	1.809(4)
M–CT	2.023(9)	2.012(6)	2.024(4)
M–C(6)	1.955(3)	1.878(17)	1.949(4)
M–C(7)	1.929(2)	1.940(16)	1.958(4)
M–P(1)	2.4542(6)	2.435(4)	2.4338(11)
C(6)–O(1)	1.162(3)	1.203(16)	1.173(5)
C(7)–O(2)	1.174(3)	1.135(15)	1.155(5)
C(6)–M–C(7)	98.51(10)	97.2(6)	81.15(17)
H(1)–M–C(6)	67.46(13)	57.2(9)	121.3(14)
H(1)–M–C(7)	65.93(13)	73.6(9)	62.8(14)
H(1)–M–P(1)	127.6(9)	126.7(9)	64.6(13)
C(6)–M–P(1)	77.70(7)	83.6(4)	82.22(12)
C(7)–M–P(1)	82.82(7)	77.6(4)	102.76(12)
CT–M–H(1)	108.9(9)	108.8(9)	116.3(12)
CT–M–C(6)	131.06(7)	126.7(5)	122.28(12)
CT–M–C(7)	125.43(7)	130.2(4)	124.53(12)
CT–M–P(1)	123.57(5)	124.07(17)	127.84(6)
M–C(1)–C(10)–C(11)	47.0(3)	50.8(17)	−47.8(5)
M–C(2)–C(20)–C(21)	162.64(15)	163.2(8)	−174.8(3)
M–C(3)–C(30)–C(31)	176.36(15)	177.0(8)	168.33(3)
M–C(4)–C(40)–C(41)	−165.59(15)	−165.8(8)	162.4(3)
M–C(5)–C(50)–C(51)	−169.60(15)	−170.7(9)	−155.5(3)
C(1)–CT–M–C(6)	23.9(6)		−54.5(2)
C(1)–CT–M–C(7)		28.8(8)	47.9(2)

CT–Cp^{Bz} centroid.

C(1)–Cp^{Bz}(centroid)–Mo(1)–C(7) of −54.5(2)° and 47.9(2)°, respectively. The Mo(1)–H(1) bond length in **3** (1.812(4) Å) is slightly longer than in **1** (1.782(3) Å). This difference may be a consequence of the trans effect caused by the PMe_3 and CO ligands in complexes **1** and **3**, respectively. In comparison with other Mo–H bond lengths determined by X-ray or neutron diffraction, ranging from 1.685(3) Å in [$MoCp_2H_2$] to 1.789(7) Å in [$MoCp^*(CO)_3H$], the Mo(1)–H(1) distance in **3** is also longer [29,30,54–57]. The distances between Mo(1)–C(6), Mo(1)–C(7) and Mo(1)–P are in the ranges usually reported in the literature.

2.2. Electrochemical studies

Electrochemical results obtained for [$MoHCp^{Bz}(CO)_2(PMe_3)$] (**1**), [$MoHCp^{Bz}(CO)_3$] (**5**), [$WHCp^{Bz}(CO)_3$] (**6**), [$WCp^{Bz}(CO)_3]_2$ (**7**), and [$MoCp^{Bz}(CO)_3(CH_3CN)]BF_4$ (**8**), using Bu_4NPF_6 as electrolyte, are summarized in Table 3.

The cyclic voltamograms of [$MHCp^{Bz}(CO)_3$] scanned in the anodic direction reveal two distinct irreversible waves at 0.72 V and 1.13 V for **5** and at 0.74 V and 1.15 V for **6**, as shown in Fig. 5a for [$MoHCp^{Bz}(CO)_3$]. When the experiment was started in the cathodic direction no reduction waves are observed in the first scan within the range of potentials available to the solvent. However, reversing of the cycle after the first scan led to the appearance of new oxidation waves at −0.57 V and −0.54 V for **5** and **6**, respectively. As is shown in Fig. 5b for **5** a subsequent cathodic scan reveals a new reduction wave with $E_p^{red}(V) = -0.95$ V. Controlled potential coulometry performed at the potential of wave I indicates that an overall transfer of two electrons takes place. The results described above are compatible with the reaction sequence presented in Scheme 1.

Following an initial oxidation to [$MHCp^{Bz}(CO)_3]^+$ (M = Mo, **5**$^+$; W, **6**$^+$) the acidity of the hydride ligands in **5**$^+$ and **6**$^+$ is greatly enhanced [24] favoring the formation of a 17-electron neutral species, [$MCp^{Bz}(CO)_3$]. The oxidation of this complex to cationic species [$MCp^{Bz}(CO)_3]^+$ justifies the second electron transfer occurring at the first wave potential. The stoichiometric balance of 2 faradays per mol revealed by the coulommetry excludes the putative formation of [$MCp^{Bz}(CO)_3]^+$ directly from [$MHCp^{Bz}(CO)_3]^+$ as it would correspond to a 1:1 metal:electron ratio. The coordination of acetonitrile to the unsaturated species leads to the solvent stabilized cation [$MCp^{Bz}(CO)_3(CH_3CN)]^+$ that is further oxidized at wave II to [$MCp^{Bz}(CO)_3(CH_3CN)]^{2+}$. An alternative explanation provided by Tilset and co-workers for analogous cyclopentadienyl

Table 3
Cyclic voltammetry data for **1**, **5**, **6**, **7** and **8**.

Compound	E_p^{ox} (I)	E_p^{ox} (II)	E_p^{red} (III)	E_p^{ox} (IV)[a]	E_p^{red}(V)	E_p^{ox}(VI)
[$MoHCp^{Bz}(CO)_2(PMe_3)$], **1**	0.26	0.74	0.16[b]	–	-1.64[c]	–
[$MoHCpBz(CO)_3$], **5**	0.72	1.13	–	-0.57	-0.95[d]	0.48[a]
[$WHCp^{Bz}(CO)_3$], **6**	0.74	1.15	–	-0.54	–	0.55[a]
[$WCp^{Bz}(CO)_3]_2$, **7**	0.55	1.24	-1.95	-0.64	–	–
[$MoCp^{Bz}(CO)_3(CH_3CN)]BF_4$, **8**	1.13	–	–	-0.57	-0.95	–

Cyclic voltammetry at 25 °C: V vs. Ferrocene/Ferrocenium couple; all potentials were evaluated at 200 mVs^{-1} in CH_3CN except for **7** where CH_2Cl_2 was used.
[a] Appears only after cathodic scan.
[b] $E^{1/2}$(red) appears upon scan reverse after II.
[c] Appears upon scan reverse after I.
[d] Appears upon scan reverse after I or IV.

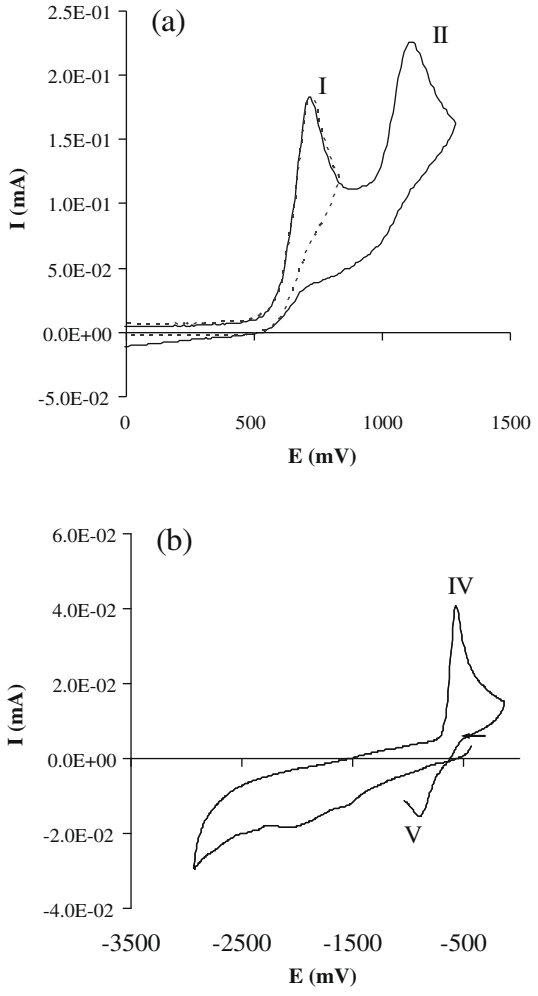

Fig. 5. Voltammogram of a solution of **5**, in CH_3CN/Bu_4NPF_6 at a vitreous carbon electrode and a scan rate of 200 mVs^{-1}, run in the anodic (a) and cathodic (b) directions.

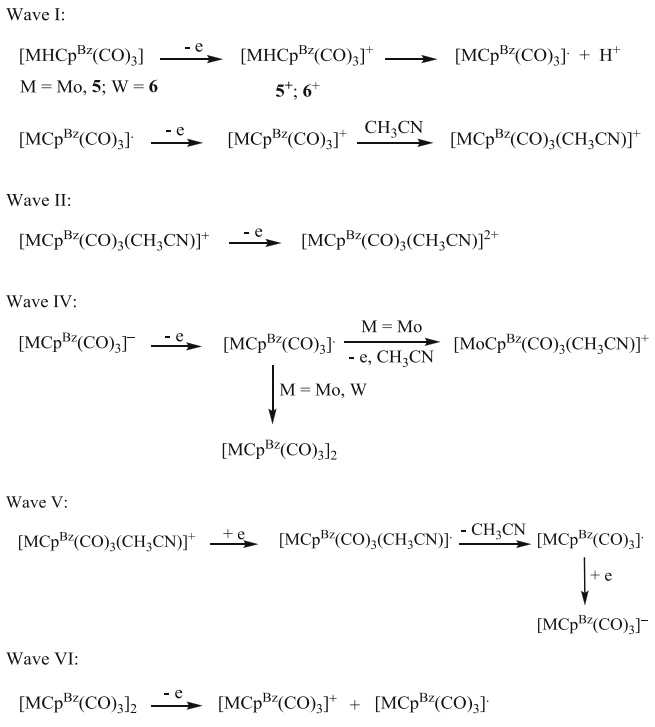

Scheme 1.

systems claims the coordination of CH_3CN and formation of 19-electron complexes prior to the oxidation reactions (Scheme 2, path i). [24,35] Even though this mechanism may not be ruled out, DFT calculations performed on cationic compounds of general formula $[MoCp'(CO)_3(L)]^+$ ($Cp' = C_5H_5$, $C_5(CH_2Ph)_5$) have shown that the stability of Cp^{Bz} derivatives is lower than that of Cp analogues [18] and one equivalent situation may be envisaged for neutral complexes, shifting the solvent coordination equilibrium towards $[MoCp^{Bz}(CO)_3]^{\cdot}$ (Scheme 2, path ii).

Chemical studies have shown that the protonation of $[MHCp'(CO)_3]$ or $[MHCp'(CO)_2(PR_3)]$ ($Cp' = C_5H_5$, Cp^{Bz}; $PR_3 = PMe_3$, PPh_3) with strong acids leads to the formation of cationic dihydrides that are unstable and, in the presence of neutral 2 electron donors, give $[MCp'(CO)_3L]^+$ or $[MCp'(CO)_2(PR_3)L]^+$ by H_2 replacement [13,18,33]. These results raise an alternative hypothesis where the starting hydride complexes would behave as possible proton acceptors from $[MHCp^{Bz}(CO)_3]^+$. $[MH_2Cp^{Bz}(CO)_3]^+$ would then be an intermediate of the formation of $[MCp^{Bz}(CO)_3(CH_3CN)]^+$ and H_2 should concomitantly be formed. The electron balance resulting from such a process would correspond to a global transfer of one electron per mol of [MH] that does not fit our experimental findings. This discrepancy between the electronic balance in chemical and electrochemical experiments has been noted by other authors (see for instance [24,33]) and has been reconciled by considering that the mechanisms operating in electrochemical and chemical conditions are different.

The definitive assignment of the oxidation process occurring at wave II was possible by comparison with the cyclic voltammogram

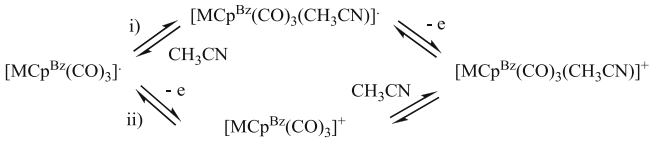

Scheme 2.

of an independently prepared sample of $[MoCp^{Bz}(CO)_3(CH_3CN)]BF_4$ (**8**), which shows an irreversible oxidation wave at the same potential (see below).

Even though the first cathodic scans of **5** and **6** do not reveal any reduction waves, the analysis of the results of subsequent cycles (see below) requires that one postulates the reduction of **5** and **6** to the corresponding 19-electron anions $[MHCp^{Bz}(CO)_3]^-$ that are converted to $[MCp^{Bz}(CO)_3]^-$. A controlled potential electrolysis performed at −1.70 V attested the transfer of one electron and the formation of H_2, identified by mass spectrometry, during the reduction process. The nonappearance of a well-defined cathodic wave reveals that the reduction of **5** and **6** occurs through a very broad wave that spreads over a large range of potentials, characteristic of a quasi-reversible electrode process that displays a low heterogeneous rate constant and a small transfer coefficient (α) [58]. The formation of H_2 may result either from an homolytic cleavage of the M–H bonds after reduction [32] or from a heterolytic process consisting in the loss of hydride from the19-electron reduced complex to the parent metal hydride. This route is consistent with the diverse reactivity of metal carbonyl hydrides, for which M–H bonds may break as a proton, a hydrogen atom or a hydride [8,9,59–62].

The oxidation process observed at wave IV (Fig. 5b) is related to the oxidation of $[MCp^{Bz}(CO)_3]^-$ to the radical $[MCp^{Bz}(CO)_3]$. Once formed, $[MCp^{Bz}(CO)_3]$ may be oxidized to $[MCp^{Bz}(CO)_3(CH_3CN)]^+$ or dimerize to $[MCp^{Bz}(CO)_3]_2$. The formation of the two compounds takes place at wave IV potential. The presence of $[MCp^{Bz}(CO)_3(CH_3CN)]^+$ is inferred from wave V that is observed upon scan reverse and assigned to its reduction. A similar reduction was observed in the cyclic voltammogram of **8** that also shows a wave at −0.95 V (see below); The formation of the dimers is revealed by small oxidation waves observed at 0.48 V for **5** and 0.55 V for **6** (wave VI) that are assigned to the oxidation of the respective dimers, in conformity with the studies of **7** described below. The lack of cationic oxidation products for **6** (wave V is absent) denotes that radical coupling is a preferred route for tungsten. The formation of $[MoCp(CO)_3]_2$ by oxidative coupling, upon controlled-potential electrolysis of $[MoHCp(CO)_3]$ in acetonitrile, was reported by Kochi as a preferential pathway [37].

The cyclic voltammograms obtained for $[MoHCp^{Bz}(CO)_2(PMe_3)]$ (**1**), in acetonitrile are presented in Fig. 6. The two irreversible anodic waves observed in Fig. 6a resemble those of Fig. 5a and are likely due to oxidation processes similar to those described for complexes **5** and **6**. The lower potentials corresponding to the oxidation waves of **1** reflect a richer metal centre, as expected upon replacement of a CO by a PMe_3 ligand. A coulometric experiment carried at the potential of wave I confirmed the transfer of 2-electrons as required for the formation of $[MoCp^{Bz}(CO)_2(PMe_3)(CH_3CN)]^+$ from **1**. This complex was isolated at the end of the experiment and identified by NMR and IR. The oxidation process responsible for the appearance of wave II is thus associated to the oxidation of $[MoCp^{Bz}(CO)_2(PMe_3)(CH_3CN)]^+$ to the dication $[MoCp^{Bz}(CO)_2(PMe_3)(CH_3CN)]^{2+}$. The transfer of one electron at this potential was confirmed by a coulometric experiment. When the voltammetric cycle is reversed immediately after wave I (Fig. 6b), only one reduction process, involving the exchange of 1 electron, is observed at −1.64 V (wave V in Fig. 6b). The reduction taking place at this potential refers to the formation of $[MoCp^{Bz}(CO)_2(PMe_3)(CH_3CN)]$ from the parent cation. This compound is a 19-electron species that readily dissociates CH_3CN leading to $[MoCp^{Bz}(CO)_2(PMe_3)]$. Further reduction of this radical is not observed possibly because an irreversible reaction takes place originating species that are not reducible within the potential range available [30,38].

The reduction processes taking place at wave III is reversible and related to the 17-electron dication $[MoCp^{Bz}(CO)_2(PMe_3)$-

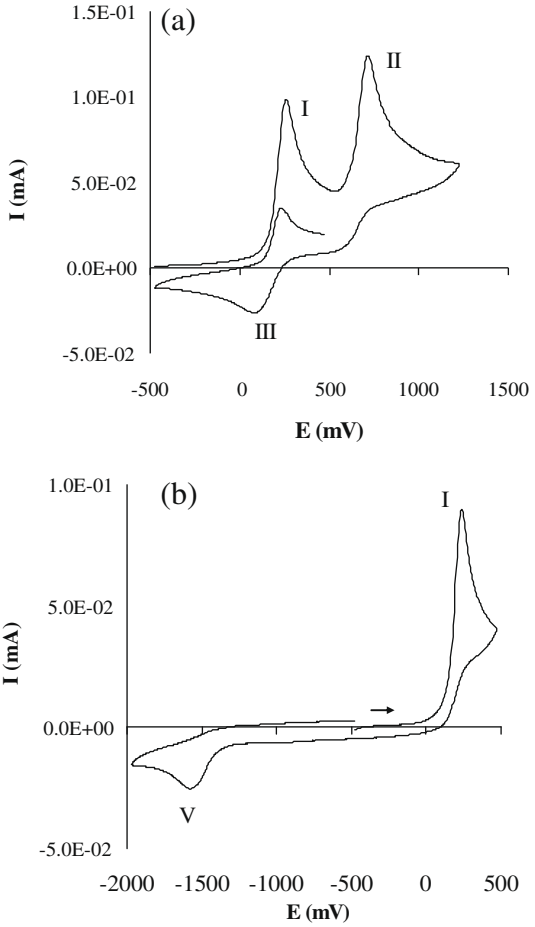

Fig. 6. Voltammogram of a solution of **1**, in CH_3CN/Bu_4NPF_6 at a vitreous carbon electrode and a scan rate of 200 mVs^{-1}, run in the anodic (a) and cathodic (b) directions.

$(CH_3CN)]^{2+}$ formed at wave II. However, the irreversibility of wave II implies that a homogeneous chemical process involving this species must take place before reduction. The first hypothesis that was considered to justify this behavior was the reaction between the $[MoCp^{Bz}(CO)_2(PMe_3)(CH_3CN)]^{2+}$ and the electrolyte anion PF_6^- [63,64]. It is well documented that BF_4^- may coordinate to molybdenum leading to the formation of zwitterionic complexes $[MoCp'(CO)_3(FBF_3)]$ ($Cp' = C_5H_5$, Cp^*, Cp^{Bz}) [18] and it has also been reported that fluorine abstraction from PF_6^- may be forced by highly acidic metal centers [65–67]. In order to check this possibility the cyclic voltammogram of **1** in CH_3CN/Bu_4NClO_4 was carried out. The result excludes the participation of the anion as the pattern observed is similar regardless of the electrolyte counter-ion.

The cyclic voltammogram of **1** in CH_2Cl_2/Bu_4NPF_6 shows that waves III and V are absent in CH_2Cl_2, which means that acetonitrile has a key role in the processes taking place at such potentials. At the present stage the nature of the process occurring at wave III remains elusive.

The electrochemistry of $[WCp^{Bz}(CO)_3]_2$ (**7**) [30], was studied in CH_2Cl_2 solutions containing Bu_4NPF_6. Two irreversible anodic peaks are observed at E_p^{ox} (I) = 0.55 V and E_p^{ox} (II) = 1.24 V. The reduction takes place through a single cathodic wave at E_p^{red} (III) = −1.95 V. The species formed in wave III is irreversibly oxidized in a subsequent anodic scan at E_p^{ox} (IV) = −0.64 V. The results obtained are consistent with the breaking of the dimer and formation of monomeric ions that participate in subsequent redox processes. The electron transfer occurring at E_p^{ox} (I) causes the weakening of the metal–metal bond and leads to the cleavage of the cationic dimer in $[WCp^{Bz}(CO)_3]^+$ and $[WCp^{Bz}(CO)_3]$. The reaction of the cation with the solvent leads to $[WCp^{Bz}(CO)_3(CH_2Cl_2)]^+$ [18] that is further oxidized at wave II to the corresponding dicationic species. The reduction of **7** also results in breaking of the metal-metal bond with formation of $[WCp^{Bz}(CO)_3]^-$ and $[WCp^{Bz}(CO)_3]$. The anion is further oxidized at −0.64 V to $[WCp^{Bz}(CO)_3]$. In accordance with the result described above for **6** (wave IV in Scheme 1), $[WCp^{Bz}(CO)_3]$ is not oxidized to $[WCp^{Bz}(CO)_3]^+$ at wave IV potential.

The oxidation of $[MoCp^{Bz}(CO)_3(CH_3CN)]BF_4$ (**8**), performed in acetonitrile with Bu_4NPF_6 as electrolyte, showed an irreversible oxidation wave at 1.13 V and a reduction wave at −0.95 V. Upon reduction and scan reverse a new anodic wave appears at −0.57 V. The anodic peak is assigned to the oxidation of **8** to $[MCp^{Bz}(CO)_3(CH_3CN)]^{2+}$ and the cathodic wave to the process $[MCp^{Bz}(CO)_3(CH_3CN)]^+/[MCp^{Bz}(CO)_3]^-$, which results from a 2-electron transfer. The wave at −0.57 V corresponds to the oxidation of $[MCp^{Bz}(CO)_3]^-$. The overall process is sequentially represented in Scheme 1 at waves V and IV.

The redox potentials obtained for pentabenzylcyclopentadienyl Mo and W complexes are, in general, consistent with results described in the literature for analogous half-sandwich complexes [24,32–34,36,38,40,41,68,69]. The comparison between the first oxidation waves of $[MCp^{Bz}(CO)_3X]$ where X = H or X = $WCp^{Bz}(CO)_3$ shows a cathodic shift for the dimer that attests for a higher metal electron density. The replacement of one CO by PMe_3 in $[MCp^{Bz}(CO)_3H]$ has a similar outcome. The results corroborate those based on the CO stretching wavenumbers of the corresponding complexes.

3. Concluding remarks

The results described show that $[MHCp^{Bz}(CO)_2(PR_3)]$ (M = Mo, W; R = Me, Ph) complexes may readily be prepared by carbonyl replacement by phosphines, but attempts to obtain the molybdenum tricyclohexylphosphine derivative led to $[Mo(CO)_4(PCy_3)_2]$ by elimination of HCp^{Bz}. Complexes $[MHCp^{Bz}(CO)_2(PR_3)]$ exist in solution as a mixture of cis and trans isomers that rapidly interconvert at room temperature. The redox potentials of $[MHCp^{Bz}(CO)_2L]$ (L = CO, PMe_3) revealed a close analogy with values previously reported for other cyclopentadienyl derivatives, pointing out that the electronic properties of the pentabenzylcyclopentadienyl ligand do not differ appreciably. However, the steric bulk of Cp^{Bz} is likely responsible for some reactivity differences observed, as the lack of prior solvent coordination in the oxidation of 17-electron species $[MCp^{Bz}(CO)_2L]$ (L = CO, PMe_3). This conclusion is attested by the similarity of the electrochemical data obtained for **5** (L = CO) in the presence and in the absence of CH_3CN, on one side, and by the formation of $[MCp^{Bz}(CO)_3]_2$ during the oxidation processes of **5** and **6**, which also reveals that formation of 19-electron species by CH_3CN coordination is disfavored in relation to cyclopentadienyl complexes.

4. Experimental section

4.1. General procedures

All manipulations were performed under a dry nitrogen atmosphere using standard Schlenk and glovebox techniques. Solvents were previously dried with 4 Å molecular sieves and distilled under a dry nitrogen atmosphere over CaH_2 (dichloromethane), P_2O_5 (acetonitrile), or sodium/benzophenone (diethyl ether and toluene). Toluene-d_8, benzene-d_6 and acetonitrile-d_3 were dried with 4 Å molecular sieves, degassed and stored under nitrogen. Literature methods were used to prepare $[MoHCp^{Bz}(CO)_3]$,

[$WHCp^{Bz}(CO)_3$] and [$WCp^{Bz}(CO)_3]_2$ [30]. PMe_3, PPh_3 and Ph_3CBF_4 were used as received from Aldrich and Bu_4NPF_6 was electrochemical grade.

NMR spectra were recorded on Bruker Avance^{II} 300 or Bruker Avance^{II} 400 spectrometers. Chemical shifts for ^1H were referenced to resonances of the residual protonated solvents relative to tetramethylsilane, and ^{13}C spectra were referenced to the solvent carbon resonance. ^{31}P spectra were referenced to external 80% H_3PO_4 (δ 0 ppm). ^{19}F spectra were referenced to external CF_3COOH (δ −76.55 ppm). ^{11}B spectra were referenced to external $BF_3{\cdot}Et_2O$ (δ 0 ppm). IR spectra were recorded as KBr pellets on a Jasco FT/IR-4100 spectrophotometer. Elemental analyses were performed at Laboratório de Análises do I.S.T., Lisbon, Portugal.

4.2. [$MoHCp^{Bz}(CO)_2(PMe_3)$] (**1**)

A 1 M solution of PMe_3 in toluene (1.0 mL, 1.00 mmol) was added dropwise to a solution of [$MoHCp^{Bz}(CO)_3$] (0.596 g, 0.86 mmol) (25 mL) in the same solvent. After stirring for 2 h at 80 °C the reaction mixture was evaporated to dryness, and extracted in diethyl ether. Concentration and cooling to −20 °C yielded yellow crystals (0.490 g, 0.65 mmol, yield 76%). ^1H NMR (C_6D_6, 25 °C, δ, ppm): 6.93–6.91 (m, 15H, *p*-C_6H_5, *m*-C_6H_5), 6.83–6.80 (m, 10H, *o*-C_6H_5), 3.84 (s, 10H, CH_2Ph), 1.10 (d, $^2J_{PH}$ = 8.6 Hz, 9H, PMe_3), −5.49 (s, 1H, Mo*H*), −5.71 (br, 1H, Mo*H*). ^{13}C NMR (C_6D_6, 25 °C, δ, ppm): 140.6 (*i*-C_6H_5), 129.2 (*o*-C_6H_5), 128.1 (*m*-C_6H_5), 126.1 (*p*-C_6H_5), 109.0 (C_5Bz_5), 33.5 (CH_2Ph), 23.0 (br, PMe_3). ^{31}P NMR (C_6D_6, 25 °C, δ, ppm): 10.9 (br, *P*Me_3). ^1H NMR (toluene-d_8, −80 °C, δ, ppm): 6.95 (br, 15H, *p*-C_6H_5, *m*-C_6H_5), 6.62 (br, 10H, *o*-C_6H_5), 3.82 (br, 10H, CH_2Ph), 1.06-1.03 (d, $^2J_{PH}$ = 7.4 Hz, 9H, PMe_3), −5.26 (d, $^2J_{PH}$ = 24.1 Hz, 1H, trans-Mo*H*), −5.57 (d, $^2J_{PH}$ = 71.2 Hz, 1H, cis-Mo*H*). ^{13}C NMR (toluene-d_8, −80 °C, δ, ppm): 141.0 (*i*-C_6H_5), 129.2 (*o*-C_6H_5), 128.1 (*m*-C_6H_5), 126.4 (*p*-C_6H_5), 109.1 (C_5Bz_5), 33.5 (CH_2Ph), 22.8 (d, $^1J_{PC}$ = 31.6 Hz, PMe_3,). ^{31}P NMR (toluene-d_8, −80 °C, δ, ppm): 19.4 (s, cis-*P*Me_3), 17.0 (s, trans-*P*Me_3). ^1H NMR (toluene-d_8, 100 °C, δ, ppm): 6.88–6.85 (m, 15H, *p*-C_6H_5, *m*-C_6H_5), 6.83–6.79 (m, 10H, *o*-C_6H_5), 3.83 (s, 10H, CH_2Ph), 1.24–1.21 (d, $^2J_{PH}$ = 8.4 Hz, 9H, PMe_3), −5.54 (d, $^2J_{PH}$ = 63.7 Hz, 1H, Mo*H*), −5.75 (d, $^2J_{PH}$ = 63.7 Hz, 1H, Mo*H*). ^{13}C NMR (toluene-d_8, 100 °C, δ, ppm): 141.3 (*i*-C_6H_5), 130.0 (*o*-C_6H_5), 128.7 (*m*-C_6H_5), 126.7 (*p*-C_6H_5), 109.7 (C_5Bz_5), 34.4 (CH_2Ph), 23.7 (d, $^1J_{PC}$ = 29.8 Hz, P*Me*3). ^{31}P NMR (toluene-d_8, - 100 °C, δ, ppm): 14.4 (s, *P*Me_3). IR (KBr pellet): $\nu_{C\equiv O}$ 1915, 1819 cm^{-1}. Anal. Calc. for $C_{45}H_{45}O_2PMo$: C, 72.57; H, 6.09. Found: C, 72.44; H, 6.32%.

4.3. [$WHCp^{Bz}(CO)_2(PMe_3)$] (**2**)

A 1 M solution of PMe_3 in toluene (1.0 mL, 1.00 mmol) was added dropwise to a solution of [$WHCp^{Bz}(CO)_3$] (0.805 g, 1.03 mmol) (25 mL) in the same solvent. The solution was refluxed overnight. The solvent was evaporated under vacuum and the residue obtained was extracted in diethyl ether. Removal of the solvent afforded a brown solid that was extracted in Et_2O. The extract was filtered, concentrated and cooled to −20 °C to afford yellow crystals (0.685 g, 0.82 mmol, yield 80%). ^1H NMR (toluene-d_8, 25 °C, δ, ppm): 6.90–6.87 (m, 15H, *p*-C_6H_5, *m*-C_6H_5), 6.75–6.72 (m, 10H, *o*-C_6H_5), 3.83 (s, 10H, CH_2Ph), 1.31 (d, $^2J_{PH}$ = 8.8 Hz, 9H, PMe_3), −7.00 (dt, $^2J_{PH}$ = 73.6 Hz, $^2J_{WH}$ = 24.9 Hz, 1H, W*H*). ^{13}C NMR (toluene-d_8, 25 °C, δ, ppm): 140.8 (*i*-C_6H_5), 129.6 (*o*-C_6H_5), 128.5 (*m*-C_6H_5), 126.5 (*p*-C_6H_5), 108.0 (C_5Bz_5), 34.1 (CH_2Ph), 24.4 (d, $^1J_{PC}$ = 34.4 Hz, PMe_3). ^{31}P NMR (toluene-d_8, 25 °C, δ, ppm): −20.8 (t, $^1J_{WP}$ = 125.2 Hz, *P*Me_3). ^1H NMR (toluene-d_8, −80 °C, δ, ppm): 6.92 (br, 15H, *p*-C_6H_5, *m*-C_6H_5), 6.58–6.56 (br m, 10H, *o*-C_6H_5), 3.83 (br, 10H, CH_2Ph), 1.18 (br d, $^2J_{PH}$ = 8.3 Hz, 9H, PMe_3), −6.52 (d, $^2J_{PH}$ = 22.6 Hz, 1H, trans-W*H*), −6.85 (dt, $^2J_{PH}$ = 72.7 Hz, $^1J_{WH}$ = 25.3 Hz, 1H, cis-W*H*). ^{13}C NMR (toluene-d_8, −80 °C, δ, ppm): 140.8 (*i*-C_6H_5), 129.2 (*o*-C_6H_5), 128.5 (*m*-C_6H_5), 126.4 (*p*-C_6H_5), 107.6 (C_5Bz_5), 33.7 (CH_2Ph), 23.4 (d, $^1J_{PC}$ = 35.0 Hz, PMe_3,). ^{31}P NMR (toluene-d_8, −80 °C, δ, ppm): −16.9 (t, $^1J_{WP}$ = 123.5 Hz, *P*Me_3), −17.6 (t, $^1J_{WP}$ = 125.2 Hz, *P*Me_3). IR (KBr pellet): $\nu_{C\equiv O}$ 1909, 1809 cm^{-1}. Anal. Calc. for $C_{45}H_{45}O_2PW$: C, 64.91; H, 5.45. Found: C, 64.36; H, 5.60%.

4.4. [$MoHCp^{Bz}(CO)_2(PPh_3)$] (**3**)

A solution of [$MoHCp^{Bz}(CO)_3$] (0.700 g, 1.0 mmol) in toluene (25 mL) was treated with PPh_3 (0.385, 1.5 mmol). After refluxing overnight, the reaction mixture was evaporated to dryness, and the oily product formed was extracted in diethyl ether. The filtered solution was concentrated and cooled at −20 °C affording yellow crystals (0.71 g, 0.76 mmol, yield 76%). ^1H NMR (toluene-d_8, 25 °C, δ, ppm): 7.70–7.66 (m, 6H, *m*-P*Ph*$_3$), 7.12–7.10 (m, 6H, *o*-P*Ph*$_3$), 7.06–7.04 (m, 3H, *p*-P*Ph*$_3$), 6.86–6.85 (m, 15H, *p*-C_6H_5, *m*-C_6H_5), 6.69–6.68 (m, 10H, *o*-C_6H_5), 3.72 (s, 10H, CH_2Ph), −4.53 (d, $^2J_{PH}$ = 69.8 Hz, 1H, Mo*H*). ^{13}C NMR (toluene-d_8, 25 °C, δ, ppm): 140.8 (*i*-C_6H_5), 138.7 (*i*-PPh_3), 133.8 (*m*-PPh_3), 129.7 (*o*-C_6H_5), 129.8 (*p*-PPh_3), 128.3 (*o*-PPh_3), 128.1 (*m*-C_6H_5), 126.4 (*p*-C_6H_5), 108.9 (C_5Bz_5), 33.7 (CH_2Ph), ^{31}P NMR (toluene-d_8, 25 °C, δ, ppm): 66.5 (s, *P*Ph_3). ^1H NMR (toluene-d_8, -50 °C, δ, ppm): 3.74 (s, 10H, CH_2Ph), −4.52 (d, $^2J_{PH}$ = 71.2 Hz, 1H, cis-Mo*H*), −5.35 (d, $^2J_{PH}$ = 20.4 Hz, 1H, trans-Mo*H*). ^{13}C NMR (toluene-d_8, −50 °C, δ, ppm): 246.93 (d, $^2J_{PC}$ = 51.07 Hz, trans-*C*O), δ 238.5 (s, cis-*C*O), ^{31}P NMR (toluene-d_8, −50 °C, δ, ppm): 72.10 (s, trans-*P*Me_3), 71.99 (s, cis-*P*Me_3). IR (KBr pellet): $\nu_{C\equiv O}$ 1932, 1847 cm^{-1}. Anal. Calc. for $C_{60}H_{51}O_2PMo$: C, 77.41; H 5.52. Found: C, 75.33; H 5.51%.

4.5. [$MoCp^{Bz}(CO)_3(CH_3CN)$]BF_4 (**8**)

A solution of Ph_3CBF_4 (0.170 g, 0.5 mmol) in CH_3CN (20 mL) was added dropwise, at −40 °C, to a solution of [$MoHCp^{Bz}(CO)_3$] (0.345 g, 0.5 mmol) (30 mL) in the same solvent. The mixture was warmed to room temperature and a red-orange solution was obtained. After stirring for 2 h, the solvent was evaporated under vacuum. The red residue was washed with hexanes (2 × 5 mL) and dried (0.395 g, 0.48 mmol, yield 96%). ^1H NMR (CD_3CN, 25 °C, δ, ppm): 7.04–7.02 (m, 15H, *p*-C_6H_5, *m*-C_6H_5), 6.82–6.80 (m, 10H, *o*-C_6H_5), 3.84(s, 10H, CH_2Ph), 2.59(s, 3H, CH_3CN). ^{13}C NMR (CD_3CN, δ, ppm): 237.5 (*C*O), 224.2 (*C*O), 138.8 (*i*-C_6H_5), 130.4 (*o*-C_6H_5), 128.7 (*m*-C_6H_5), 127.9 (*p*-C_6H_5), 118.3 (CH_3CN), 116.8 (C_5Bz_5), 32.4 (CH_2Ph), 2.1 (CH_3CN). ^{11}Br NMR (CD_3CN, δ, ppm): 3.9 (br, BF_4^-). ^{19}F NMR (CD_3CN, δ, ppm): −150.6 (br, BF_4^-). IR (KBr pellet): $\nu_{C\equiv O}$ 2070, 1993, 1976 cm^{-1}; $\nu_{C\equiv N}$ 2321, 2289 cm^{-1}; ν_{BF4} 1054 cm^{-1}.

4.6. General procedures for electrochemistry

Cyclic voltammetric and controlled potential coulometry measurements were carried out using a Radiometer DEA 101 Digital Electrochemical Analyser interfaced with an IMT 102 Electrochemical Interface. For cyclic voltammetry measurements a three-electrode cell with a total volume of around 5 mL was used. A Platinum disc (Φ = 1.5 mm) or vitreous carbon electrodes (Φ = 3.0 mm) were used as working electrodes, the counter-electrode was a Pt wire and a silver wire was used as a pseudo-reference electrode; this electrode was kept in a separate compartment and connected to the main compartment by a Luggin capillary. The ferrocene/ferrocenium couple was used as internal standard to measure wave potentials, according to IUPAC recommendations [70].

The controlled potential electrolysis electrochemical cell had a three compartment design. A large platinum gauze electrode was employed as working electrode. The pseudo-reference electrode was similar to the one used for cyclic voltammetry measurements

and it was also connected to the main compartment by a Luggin capillary. The counter electrode was also a platinum gauze electrode and it was kept in a different compartment which was connected to the main compartment by a sintered glass.

Concentrations of electrolyte around 0.2 M were used for cyclic voltammetry and 0.3 M for electrolysis experiments. Concentrations around 3×10^{-3} M (for electrolysis experiments) and around 1.2×10^{-3} M (for cyclic voltammetry) were used for the complexes being studied. All experiments were carried out at 25 °C in the absence of oxygen. Dry nitrogen was bubbled through the solution in the cell before all the measurements.

4.7. Electrolyses of $[MoHCp^{Bz}(CO)_3]$. Identification of H_2

The controlled potential electrolysis of **5** was carried out in CH_3CN/Bu_4NPF_6. After the end of the experiment, a gas phase analysis was performed with a mass detector (QMS 200 from Balzers), checking the intensity of the following fragments: m/e = 2 (H_2), = 18 (H_2O), = 28 (N_2), = 32 (O_2), = 44 (Ar).

4.8. Electrolyses of $[MoHCp^{Bz}(CO)_2(PMe_3)]$. Identification of $[MoCp^{Bz}(CO)_2(PMe_3)(CH_3CN)]PF_6$

The controlled potential electrolysis of **1** was carried out in CH_3CN/Bu_4NPF_6. After the end of the experiment the mixture was evaporated to dryness and the solid obtained was extracted in CH_2Cl_2 and filtered. The product was obtained from this solution upon concentration and addition of Et_2O. ^{1}H NMR (C_6D_6): δ 6.86–6.84 (m, 15H, *p*-C_6H_5, *m*-C_6H_5), 6.74–6.72 (m, 10H, *o*-C_6H_5), 3.64 (d, $^2J_{PH}$ = 4 Hz, 10H, CH_2Ph), 2.16 (d, $^2J_{PH}$ = 4 Hz, 3H, CH_3CN), 1.48 (d, $^2J_{PH}$ = 8 Hz, 9H, PMe_3); ^{1}H NMR (CD_3CN): δ 7.00–6.97 (m, 15H, *p*-C_6H_5, *m*-C_6H_5), 6.74-6.71 (m, 10H, *o*-C_6H_5), 3,78 (s, 10H, CH_2Ph), 1.71 (d, $^2J_{PH}$ = 9.7 Hz, 9H, PMe_3); ^{13}C NMR δ: 139.0 (*i*-C_6H_5), 129.9 (*o*-C_6H_5), 129.1 (*m*-C_6H_5), 127.4 (*p*-C_6H_5), 113.3 (C_5Bz_5), 33.1 (CH_2Ph), 16.3 (d, J_{PC} = 30.3 Hz, P(CH_3)$_3$). ^{31}P NMR, δ 3.93 (PMe_3). IR ν_{CO}: 1972, 1894 cm^{-1}.

4.9. X-ray diffraction experimental determination

Crystallographic and experimental details of crystal structure determinations are listed in Table 4. Crystals were selected, covered with polyfluoroether oil, and mounted on a nylon loop. Data was collected using graphite monochromated Mo Kα radiation (λ = 0.71073 Å) on a Bruker AXS-KAPPA APEX II diffractometer equipped with an Oxford Cryosystems open-flow nitrogen cryostat, at 150 K. Cell parameters were retrieved using Bruker SMART software and refined using Bruker SAINT on all observed reflections [71]. Absorption corrections were applied using SADABS [72]. Structure solution and refinement were performed using direct methods with the programs SIR97 [73] and SHELXL [74] both included in the package of programs WINGX-Version 1.70.01 [75]. For compound **2**, the poor diffracting power, prevented the anisotropic refinement of all the non-hydrogen atoms. This refinement would lead to a very poor ratio of "number of refined parameters/number of reflections" thus preventing a good, stable and reliable refinement. So only W, P, O and C atoms (of CO and PCH3 groups) were refined anisotropically. All hydrogen atoms, except the hydrides H atom, were inserted in idealized positions and allowed to refine riding in the parent carbon atom. Figures were generated using ORTEP3 [76]. Data was deposited in CCDC under the deposit numbers CCDC 751582, 751583, 751584 for **1**, **2** and **3,** respectively.

Table 4
Crystal data and structure refinement for **1**, **2** and **3**.

	$[MoCp^{Bz}(CO)_2(PMe_3)H]$ **1**	$[WCp^{Bz}(CO)_2(PMe_3)H]$ **2**	$[MoCp^{Bz}(CO)_2(PPh_3)H]$ **3**
Formula	Mo C_{45} H_{45} O_2 P	W C_{45} H_{45} O_2 P	Mo C_{43} H_{36} O_3
Formula weight	744.72	832.63	1005.04
T (K)	150(2)	298(2)	150(2)
λ (Å)	0.71073	0.71073	0.71073
Crystal system	monoclinic	monoclinic	triclinic
Space group	$P2_1/c$	$P2_1/c$	$P\bar{1}$
a (Å)	19.9588(3)	19.888(3)	12.891(2)
b (Å)	16.8617(5)	16.866(2)	14.264(2)
c (Å)	11.1062(6)	11.0510(17)	15.030(3)
α (°)			101.098(7)
β (°)	96.945(2)	97.085(5)	105.920(8)
γ (°)			95.604(7)
V (Å^3)	3710.2(2)	3678.5(10)	2574.7(8)
Z	4	4	2
$D_{Calc.}$ (g cm^{-3})	1.333	1.503	1.296
Absorption coefficient (mm^{-1})	0.433	3.221	0.333
F(0 0 0)	1552	1680	1052
Crystal size (mm)	0.2 × 0.2 × 0.2	0.2 × 0.2 × 0.2	0.05 × 0.10 × 0.20
Crystal morphology	cube	cube	prism
Colour	yellow	yellow	yellow
θ (°)	1.03–31.71	1.59–19.87	1.45–26.55
Limiting indices	$-29 \leqslant h \leqslant 29$; $-24 \leqslant k \leqslant 23$; $-16 \leqslant l \leqslant 16$	$-18 \leqslant h \leqslant 18$; $-15 \leqslant k \leqslant 15$; $-10 \leqslant l \leqslant 10$	$-16 \leqslant h \leqslant 16$; $-17 \leqslant k \leqslant 17$; $-18 \leqslant l \leqslant 18$
Reflections collected/ unique (R_{int})	55443/12353 (0.0581)	15051/3287 (0.0934)	40253/10521 (0.0919)
Completeness to θ	98.1% (θ = 31.71°)	97.6% (θ = 19.87°)	98.2% (θ = 26.55°)
Refinement method	full-matrix least-squares on F^2	full-matrix least-squares on F^2	full-matrix least-squares on F^2
Data/ restraints/ parameters	12353/0/446	3287/54/247	10521/0/626
Goodness of fit on F^2	1.074	0.986	1.019
Final R indices [$I > 2\sigma(I)$]	$R1$ = 0.0473, $wR2$ = 0.1130	$R1$ = 0.0542, $wR2$ = 0.1313	$R1$ = 0.0526, $wR2$ = 0.1140
R indices (all data)	$R1$ = 0.0774, $wR2$ = 0.1296	$R1$ = 0.0852, $wR2$ = 0.1450	$R1$ = 0.0949, $wR2$ = 0.1478
Largest difference peak/hole (e Å^{-3})	3.099 e–0.889	1.988 e–1.459	0.486 e–0.996

Acknowledgements

The authors are grateful to Fundação para a Ciência e a Tecnologia, Portugal, for funding (PPCDT/QUI/55744/2004, PTDC/QUI/66187/2006 and SFRH/BPD/26745/2006)

Appendix A. Supplementary material

CCDC 751582, 751583, 751584 contain the supplementary crystallographic data for this paper. These data can be obtained free of charge from The Cambridge Crystallographic Data Centre via www.ccdc.cam.ac.uk/data_request/cif. Supplementary data associated with this article can be found, in the online version, at doi:10.1016/j.jorganchem.2010.02.012.

References

[1] (a) A. Börner, J. Holz, in: M. Beller, C. Bolm (Eds.), Transition Metals for Organic Synthesis, second ed., vol. 2, Wiley-VCH, 2004, pp. 3–28;
(b) T. Ohkuma, R. Noyori, in: M. Beller, C. Bolm (Eds.), Transition Metals for Organic Synthesis, second ed., vol. 2, Wiley, VCH, 2004, pp. 29–113;
(c) F. Spindler, H.U. Blaser, in: M. Beller, C. Bolm (Eds.), Transition Metals for

Organic Synthesis, 2nd ed., vol. 2, Wiley-VCH, pp. 113–123;
(d) H.-U. Blaser, H. Steiner, M. Studer, in: M. Beller, C. Bolm (Eds.), Transition Metals for Organic Synthesis, second ed., vol. 2, Wiley-VCH, 2004, pp. 125–143;
(e) S. Gladiali, E. Alberico, in: M. Beller, C. Bolm (Eds.), Transition Metals for Organic Synthesis, vol. 2, second ed., Wiley-VCH, 2004, pp. 145–166.
[2] J. Choi, M.E. Pulling, D.M. Smith, J.R. Norton, J. Am. Chem. Soc. 130 (2008) 4250.
[3] W.W. Ellis, J.W. Raebiger, C.J. Curtis, J.W. Bruno, D.L. DuBois, J. Am. Chem. Soc. 126 (2004) 2738.
[4] W.W. Ellis, R. Ciancanelli, S.M. Miller, J.W. Raebiger, M.R. DuBois, D.L. DuBois, J. Am. Chem. Soc. 125 (2003) 12230.
[5] H. Jacobsen, H. Berke, in: M. Peruzzini, R. Poli (Eds.), Recent Advances in Hydride Chemistry, Elsevier, 2001, pp. 89–116.
[6] N. Sarker, J.W. Bruno, J. Am. Chem. Soc. 121 (1999) 2174.
[7] R.J. Angelici, Acc. Chem. Res. 28 (1995) 51.
[8] S.S. Kristjánsdóttir, J.R. Norton (Eds.)A. Didieu (Ed.), Transition Metal Hydrides, Wiley-VCH, 1991, pp. 309–359.
[9] (a) M. Tilset, V.D. Parker, J. Am. Chem. Soc. 111 (1989) 6711;
(b) M. Tilset, V.D. Parker, J. Am. Chem. Soc. 112 (1990) 2843.
[10] T.-Y. Cheng, R.M. Bullock, Organometallics 21 (2002) 2325.
[11] T.-Y. Cheng, B.S. Brunschwig, R.M. Bullock, J. Am. Chem. Soc. 120 (1998) 13121.
[12] D.C. Eisenberg, C.J.C. Lawrie, A.E. Moody, J.R. Norton, J. Am. Chem. Soc. 113 (1991) 4888.
[13] J.-S. Song, D.J. Szalda, R.M. Bullock, Organometallics 20 (2001) 3337.
[14] J.-S. Song, R.M. Bullock, J. Am. Chem. Soc. 116 (1994) 8602.
[15] J.-S. Song, D.J. Szalda, R.M. Bullock, C.J.C. Lawrie, M.A. Rodkin, J.R. Norton, Angew. Chem., Int. Ed. 31 (1992) 1233.
[16] D.N. Kursanov, Z.N. Parnes, N.M. Loim, Synthesis (1974) 633.
[17] K.-T. Smith, J.R. Norton, M. Tilset, Organometallics 15 (1996) 4515.
[18] S. Namorado, M.A. Antunes, L.F. Veiros, J.R. Ascenso, M.T. Duarte, A.M. Martins, Organometallics 27 (2008) 4589.
[19] H. Guan, M. Limura, M.P. Magee, J.R. Norton, G. Zhu, J. Am. Chem. Soc. 127 (2005) 7805.
[20] R.M. Bullock, Chem. Eur. J. 10 (2004) 2366.
[21] M.P. Magee, J.R. Norton, J. Am. Chem. Soc. 123 (2001) 1778.
[22] M.H. Voges, R.M. Bullock, J. Chem. Soc., Dalton Trans. (2002) 759.
[23] B.F.M. Kimmich, P.J. Fagan, E. Hauptman, W.J. Marshall, R.M. Bullock, Organometallics 24 (2005) 6220.
[24] O.B. Ryan, M. Tilset, V.D. Parker, J. Am. Chem. Soc. 112 (1990) 2618.
[25] N.V. Belkova, M. Besora, M. Baya, P.A. Dub, L.M. Epstein, A. Lledós, R. Poli, P.O. Revin, E.S. Shubina, Chem. Eur. J. 14 (2008) 9921.
[26] N.V. Belkova, E.I. Gutsul, O.A. Filippov, V.A. Levina, D.A. Valyaev, L.M. Epstein, A. Lledós, E.S. Shubina, J. Am. Chem. Soc. 128 (2006) 3486.
[27] L.M. Epstein, E.S. Shubina, Coord. Chem. Rev. 231 (2002) 165.
[28] J.C. Fettinger, H.-B. Kraatz, Rinaldo Poli, E.A. Quadrelli, R.C. Torralba, Organometallics 17 (1998) 5767.
[29] M. Baya, P.A. Dub, J. Houghton, J.-C. Daran, N.V. Belkova, E.S. Shubina, L.M. Epstein, A. Lledós, R. Poli, Inorg. Chem. 48 (2009) 209.
[30] S. Namorado, J. Cui, C.G. de Azevedo, M.A. Lemos, M.T. Duarte, J.R. Ascenso, A.R. Dias, A.M. Martins, Eur. J. Inorg. Chem. (2007) 1103.
[31] T.-Y. Cheng, D.J. Szalda, J. Zhang, R.M. Bullock, Inorg. Chem. 45 (2006) 4712.
[32] M.-L. Marcos, C. Moreno, R.M. Medina, M.-J. Macazaga, S. Delgado, J. González-Velasco, J. Organomet. Chem. 568 (1998) 185.
[33] E.A. Quadrelli, H.-B. Kraatz, R. Poli, Inorg. Chem. 35 (1996) 5154.
[34] D.C. Barbini, P.S. Tanner, T.D. Francone, K.B. Furst, W.E. Jones Jr., Inorg. Chem. 35 (1996) 4017.
[35] M. Tilset, Inorg. Chem. 33 (1994) 3121.
[36] V. Skagestad, M. Tilset, J. Am. Chem. Soc. 115 (1993) 5077.
[37] R.J. Klingler, J.C. Huffman, J.K. Kochi, J. Am. Chem. Soc. 102 (1980) 208.
[38] K.-T. Smith, M. Tilset, J. Organomet. Chem. 431 (1992) 55.
[39] V. Skagestad, M. Tilset, Organometallics 11 (1992) 3293.
[40] K.M. Kadish, D.A. Lacombe, J.E. Anderson, Inorg. Chem. 25 (1986) 2246.
[41] R. Moulton, T.W. Weidman, K.P.C. Vollhardt, A.J. Bard, Inorg. Chem. 25 (1986) 1846.
[42] D. Astruc, Chem. Rev. 88 (1988) 1189.
[43] A.M. Martins, C.C. Romão, M. Abrantes, M.C. Azevedo, J. Cui, A.R. Dias, M.T. Duarte, M.A. Lemos, T. Lourenço, R. Poli, Organometallics 24 (2005) 2582.
[44] A.M. Martins, R. Branquinho, J. Cui, A.R. Dias, M.T. Duarte, J. Fernandes, S.S. Rodrigues, J. Organomet. Chem. 689 (2004) 2368.
[45] P. Kalck, R. Pince, R. Poilblanc, J. Roussel, J. Organomet. Chem. 24 (1970) 445.
[46] H.G. Halt, H.E. Engelhardt, W. Klaui, A. Muller, J. Organomet. Chem. 331 (1987) 317.
[47] P. Kalck, R. Poilblanc, J. Organomet. Chem. 19 (1969) 115.
[48] A. Bainbrid, P.J. Craig, M. Green, J. Chem. Soc. 11 (1968) 2715.
[49] S.P. Nolan, R.L. de laVega, S.L. Mukerjee, C.D. Hoff, Inorg. Chem. 25 (1986) 1160.
[50] E.C. Alyea, G. Ferguson, S. Kannan, Acta Crystallogr. Sect. C 52 (1996) 765.
[51] F.H. Allen, W.D.S. Motherwell, Acta Crystallogr. Sect. B 58 (2002) 407.
[52] (a) P. Kubácek, R. Hoffman, Z. Havlas, Organometallics 1 (1982) 180;
(b) R. Poli, Organometallics 9 (1990) 1892.
[53] L.-C. Song, L.-Y. Zhang, Q.-M. Hu, X.-Y. Huang, Inorg. Chim. Acta 230 (1995) 127.
[54] M. Baya, J. Houghton, J.-C. Daran, R. Poli, L. Male, A. Albinati, M. Gutman, Chem. Eur. J. 13 (2007) 5347.
[55] A.J. Schultz, K.L. Stearley, J.M. Williams, R. Mink, G.D. Stucky, Inorg. Chem. 16 (1977) 3303.
[56] L. Brammer, D. Zhao, R.M. Bullock, R.K. McMullan, Inorg. Chem. 32 (1993) 4819.
[57] Y.-C. Tsai, M.J.A. Johnson, D.J. Mindiola, C.C. Cummins, J. Am. Chem. Soc. 121 (1999) 10426.
[58] A.J. Bard, L.R. Faulkner, Electrochemical Methods: Fundamentals and Applications, second ed., John-Wiley and Sons, New York, 2001. p. 237.
[59] T.-Y. Cheng, R.M. Bullock, Organometallics 14 (1995) 4031.
[60] E.T. Papish, M.P. Magee, J.R. Norton, in: M. Peruzzini, R. Poli (Eds.), Recent Advances in Hydride Chemistry, Elsevier, 2001, pp. 39–74.
[61] L.M. Epstein, N.V. Belkova, E.S. Shubina, in: M. Peruzzini, R. Poli (Eds.), Recent Advances in Hydride Chemistry, Elsevier, 2001, pp. 391–418.
[62] J.M. O'Connor, S.J. Friese, Organometallics 27 (2008) 4280.
[63] F. Barrière, R.U. Kirss, W.E. Geiger, Organometallics 24 (2005) 48.
[64] B.L. Ghent, S.L. Martinak, L.A. Sites, J.A. Golen, A.L. Rheingold, C. Nataro, J. Organomet. Chem. 692 (2007) 2365.
[65] M.A. Alvarez, G. Garcia, M.E. Garcia, V. Riera, M.A. Ruiz, Organometallics 18 (1999) 4509.
[66] R.V. Honeychuck, W.H. Hersch, Inorg. Chem. 28 (1989) 2869.
[67] W. Beck, K. Sunkel, Chem. Rev. 88 (1988) 1405.
[68] J.R. Pugh, T.J. Meyer, J. Am. Chem. Soc. 114 (1992) 3784.
[69] A. Asdar, M.J. Tudoret, C. Lapinte, J. Organomet. Chem. 349 (1988) 353.
[70] G. Gritzer, J. Kuta, J. Electrochim. Acta 29 (1984) 869.
[71] SMART and SAINT: Area Detector Control and Integration Software, Bruker AXS, 2004, Madison, WI, USA.
[72] G.M. Sheldrick, SADABS, Program for Empirical Absorption Correction of Area Detectors (Version 2.10), University of Göttingen, Germany, 2004.
[73] A. Altomare, M.C. Burla, M. Camalli, G.L. Cascarano, C. Giacovazzo, A. Guagliardi, A.G.G. Moliterni, G. Polidori, R. Spagna, J. Appl. Crystallogr. 32 (1999) 115.
[74] G.M. Sheldrick, SHELXL-97 a Computer Program for the Refinement of Crystal Structures, University of Göttingen, Göttingen, Germany, 1997.
[75] L.J. Farrugia, J. Appl. Crystallogr. 32 (1999) 837.
[76] L.J. Farrugia, J. Appl. Crystallogr. 30 (1997) 565.